

# Graph is a Substrate Across Data Modalities

Ziming Li<sup>1</sup> Xiaoming Wu<sup>2</sup> Zehong Wang<sup>3</sup> Jiazheng Li<sup>1</sup> Yijun Tian<sup>3</sup>  
 Jinhe Bi<sup>4</sup> Yunpu Ma<sup>4</sup> Yanfang Ye<sup>3</sup> Chuxu Zhang<sup>1†</sup>

## Abstract

Graphs provide a natural representation of relational structure that arises across diverse domains. Despite this ubiquity, graph structure is typically learned in a modality- and task-isolated manner, where graph representations are constructed within individual task contexts and discarded thereafter. As a result, structural regularities across modalities and tasks are repeatedly reconstructed rather than accumulated at the level of intermediate graph representations. This motivates a representation-learning question: *how should graph structure be organized so that it can persist and accumulate across heterogeneous modalities and tasks?* We adopt a representation-centric perspective in which graph structure is treated as a structural substrate that persists across learning contexts. To instantiate this perspective, we propose **G-Substrate**, a graph **substrate** framework that organizes learning around shared graph structures. G-Substrate comprises two complementary mechanisms: a unified structural schema that ensures compatibility among graph representations across heterogeneous modalities and tasks, and an interleaved role-based training strategy that exposes the same graph structure to multiple functional roles during learning. Experiments across multiple domains, modalities, and tasks show that G-Substrate outperforms task-isolated and naive multi-task learning methods.

## 1. Introduction

Graphs provide a natural abstraction for relational information and arise across a wide range of domains and learning problems. For example, in computer vision, scene graphs encode objects and their interactions (Chen et al., 2024d; Li et al., 2024a); in natural language processing, event graphs

<sup>1</sup>University of Connecticut <sup>2</sup>National University of Singapore  
<sup>3</sup>University of Notre Dame <sup>4</sup>LMU Munich. Correspondence to: Chuxu Zhang <chuxu.zhang@uconn.edu>.

Preprint. February 2, 2026.

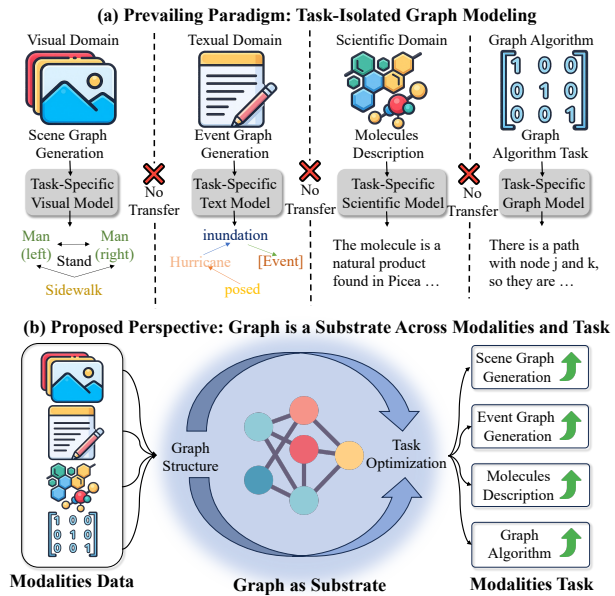


**Figure 1. Task-isolated graph modeling vs. graph structure as a substrate.** (a) Graph structure is learned in task-isolated pipelines, causing structurally similar graph patterns to occupy separate representation regions and limit cross-modal interaction. (b) We organize graph structure as a shared substrate, encouraging graph patterns from different data modalities to converge and align, so structurally analogous configurations can mutually shape the representation and improve performance.

organize temporal and causal relations (Hu et al., 2025e; Xu et al., 2025b); in chemistry, molecular graphs represent atoms and bonds (Kim et al., 2025; Liu et al., 2024c); and in graph algorithmic tasks, graphs underlie tasks such as connectivity, shortest paths, and structural reasoning (Wang et al., 2025b; Hu et al., 2025c). Despite differences in input modalities and task objectives, graph structure provides an explicit structural interface through which heterogeneous data modalities can be organized (Wang et al., 2025f).

However, the widespread presence of graph-structured representations across tasks and modalities does not imply that learning systems are organized to preserve or accumulate graph structure. In practice, graph structure is built to serve a single objective and discarded after training, as shown in Figure 1(a). Many existing approaches instantiate structure through task-specific graph representations, for example, as supervision targets in scene graph generation (Wu et al.,

2025a; Liu et al., 2025) or event relation extraction (Tao et al., 2025; Zhao et al., 2025c), even when structurally similar graph patterns arise from different input modalities. Recent efforts that aim to unify graph-centric learning largely focus on expanding task coverage or sharing model architectures, but still treat graph structure as a task-bound input or output rather than as a persistent intermediate state (Sun et al., 2025; Wang et al., 2024e;b; He et al., 2024). These approaches are architecture-centric: they share model components, but do not establish a graph-level representation state that persists across tasks (Standley et al., 2020; Ruder, 2017). As a result, relational regularities found in one setting do not accumulate at the level of the graph, but remain confined to task-specific formulations. This exposes a representation-level mismatch: graph structure is treated as task-specific data rather than as a persistent learning state.

The above issue motivates the following question: *how should graph structure be organized so that it can persist and accumulate across heterogeneous learning contexts rather than being reconstructed independently in each task?* Moreover, we do not attempt to unify task semantics but rather to align structural patterns that recur across domains.

There are two factors that prevent graph structure from functioning as a reusable intermediate state. First, graph structure varies widely across modalities and tasks in schema, granularity, and representational form. This heterogeneity prevents direct reuse of graphs across learning contexts and makes structural compatibility across graph representations a prerequisite for reuse (Xu et al., 2025a; Chai et al., 2025). Second, graph representations participate in learning under different functional roles: some tasks construct or refine graph structure, while others rely on it for reasoning, prediction, or evaluation. A reusable intermediate graph representation must therefore remain functional under both structure-generate (Lafferty et al., 2001; Zellers et al., 2018) and structure-understand roles (Battaglia et al., 2018; Hamilton et al., 2017). By this cross-role requirement, a structural constraint is introduced that encourages representations that remain robust and usable across tasks, rather than those over-specialized to a single objective.

Therefore, in this paper, we introduce a representation-centric view which considers *graph structure as a persistent intermediate substrate* for coordinating learning across data modalities and functional roles, as shown in Figure 1(b). To operationalize this perspective, we introduce G-Substrate, a framework built around two complementary mechanisms: a *unified structural schema* that establishes compatibility of graph representations across tasks and modalities, and *interleaved role-based training* that exposes the same graph to multiple functional roles during learning. These mechanisms address structural and role heterogeneity, respectively.

We evaluate G-Substrate across tasks from multiple domains

and modalities and show that it consistently outperforms task-isolated training and naive multi-task baselines. Importantly, both structural alignment and cross-role exposure contribute to performance, while their combination leads to the strongest improvements. This suggests that the most robust graph representations emerge when structural alignment is combined with role-based training.

## 2. The G-Substrate Framework

This section presents the G-Substrate framework and describes how the substrate-oriented perspective is realized in both data representation and model learning. Specifically, we formalize the central perspective of this work: *graph structure as a persistent substrate rather than a task-bound artifact* (Section 2.1). This perspective leads to two design requirements, namely structural compatibility and cross-role reuse, which together define the design space of the framework. We address the first requirement by organizing graphs within a unified graph state space, aligning representations from heterogeneous tasks into a common structural form (Section 2.2). We address the second requirement through interleaved role-based supervision, a training organization that exposes graph to multiple functional roles and promotes their reuse across learning contexts (Section 2.3).

### 2.1. Perspective: Graph is a Structural Substrate

Graph structure arises across a wide range of learning problems, but is most often modeled in a task-bound manner. In many settings, such a structure is made explicit through graph representations. In prevailing practice, graph representations are constructed to serve individual task objectives and discarded thereafter, causing structural regularities that recur across tasks and modalities to be repeatedly reconstructed in isolation. In contrast, we introduce a new representation-centric perspective: *graph is a reusable structural substrate across data modalities*. Building on this perspective, we propose G-Substrate, a framework that organizes learning contexts across domains and modalities.

To empirically support this perspective, we examine whether structurally similar graph configurations recur across heterogeneous tasks and whether they play comparable structural roles despite differences in task semantics. We provide evidence for this perspective through quantitative structural statistics and qualitative motif analysis across heterogeneous domains, as reported in Table 1. These statistics summarize coarse topological properties, including average degree (AvgDeg), average shortest path length (ASPL), and the prevalence of simple local motifs such as two-hop chains and hub-centered patterns. Although global graph properties differ substantially, coarse local structures recur with non-trivial frequency in all settings studied. Beyond their prevalence, these graph structures play aligned functional roles. Figure 2 shows a hub-centered configuration in an

event graph and a scene graph. In the former, the event *received* participates in multiple temporal dependencies; in the latter, the object *horse* participates in multiple spatial relations. While task semantics differ, the central node in both cases coordinates multiple edges and constrains how they compose, indicating cross-domain invariance at the level of graph structure rather than task-specific meaning. These observations are drawn from representative datasets in scene graph generation, event relation extraction, molecular graphs, and algorithmic graph tasks, with detailed dataset descriptions and measurements provided in Appendix A.

*Table 1.* Coarse topology statistics (per-graph averages). While global structural scale differs, recurring local structures are observed across all domains.

Domain	AvgDeg	ASPL	TwoHop	Hubs
Graph algorithm	5.8	2.1	633	16
Molecular graphs	2.1	6.2	53	12
Scene graphs	1.5	1.4	2.4	0.7
Event graphs	1.5	1.4	15	0.9

[1] The Last Girl on Earth Tour was the third concert tour ... [2] The tour visited Europe ... [3] The tour was announced through ... [4] In the interview, Rihanna stated... [5] The tour received generally ... Task: Given the document and the pre-annotated events, output ALL relations ...

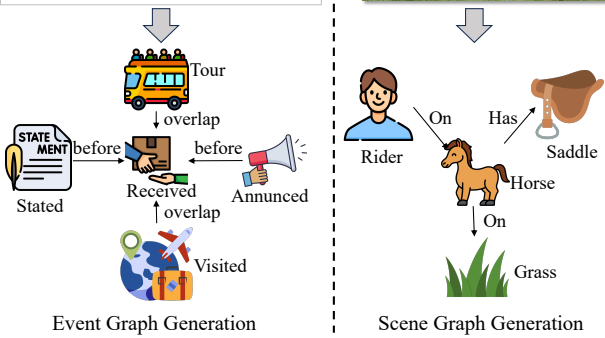


*Figure 2.* Analogous constraint roles of hub motifs across tasks. In the event graph, the hub event *received* participates in multiple temporal dependencies; in the scene graph, the hub object *horse* participates in multiple spatial relations. The central node coordinates multiple relations and constrains their joint consistency.

To formalize this substrate-oriented view, we treat a graph as the fundamental structural representation. Specifically, a graph is defined as a set of structural triples  $G = \{(u, r, v)\}$ , where  $u$  and  $v$  denote entities and  $r$  denotes a typed edge between them. Crucially, a graph excludes task-specific semantics, execution logic, and optimization objectives; its identity is determined solely by the structural configuration it encodes. Optionally, entities or edges may be associated with attributes, which are treated as auxiliary annotations and do not alter the underlying relational structure.

The graph substrate perspective treats graph as an inter-

mediate structural representation intended to persist across learning contexts. For a graph to serve this role, two requirements follow. First, graphs arising from different learning settings must be structurally compatible so that they can reside in a unified representation space. Second, training must explicitly support the reuse of graphs across functional roles, rather than confining them to task-local roles. G-Substrate operationalizes these requirements through a unified structural schema and an interleaved cross-task training strategy.

## 2.2. Structural Compatibility: A Unified Schema

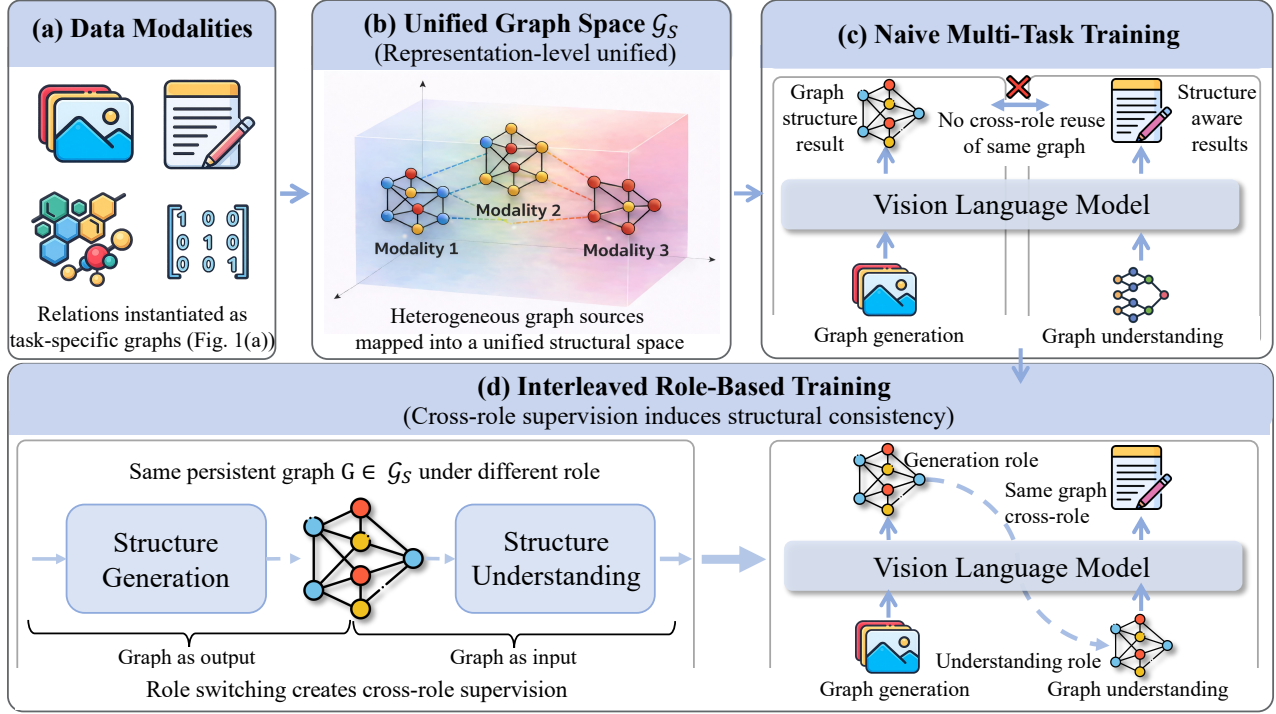
To ensure structural compatibility across tasks, G-Substrate organizes graphs in a *unified graph state space*. Building on the graph definition in Section 2.1, we denote this space as  $\mathcal{G}_s = \{G \mid G = \{(u, r, v)\}\}$ , where each  $G \in \mathcal{G}_s$  consists of entities  $u, v$  connected by typed edges  $r$ . Graphs arising from different modalities and tasks are mapped into this common structural space, sharing consistent node identifiers, edge types, and connectivity rules. Figure 2 gives examples of this mapping. An event graph constructed from text and a scene graph constructed from an image are both represented as graph instances  $G \in \mathcal{G}_s$ . Although originating from different modalities and tasks, these graphs share the same structural form, making hub-centered structural patterns (e.g., *received* and *horse* in the figure) comparable in  $\mathcal{G}_s$ .

Figure 3(b) provides a geometric intuition for this alignment. Graphs from different modalities and tasks may initially occupy disjoint regions under task-specific conventions. Expressing them in the unified graph state space  $\mathcal{G}_s$  brings these heterogeneous constructions into a common structural region, where structurally compatible patterns become aligned. Importantly, this concentration arises from explicit structural representation alignment rather than from parameter sharing or feature similarity alone.

Structural compatibility alone, however, does not guarantee that graphs are meaningfully exercised under diverse functional roles during learning. Even in a shared structural space, a graph may still be optimized only in a single usage context. Enabling unified graph representations to function consistently across roles and tasks therefore requires an appropriate training organization, which is provided by the interleaved role-based training described next.

## 2.3. Cross-task Reuse: Interleaved Role-based Training

A unified graph state space establishes structural compatibility of graphs across tasks, but does not by itself determine how those graphs are used during learning. Under naive multi-task training, different tasks are optimized jointly using a shared backbone model, with each task receiving its native modality input and producing task-specific outputs under its own objective. A common instantiation of this naive setup is to use a single vision–language foundation model as a shared backbone to process heterogeneous



**Figure 3. Unified graph substrate and cross-role training.** Graph structures from heterogeneous modalities are mapped into a unified graph state space  $\mathcal{G}_S$ , where graphs serve as persistent structural representations (b). Under naive multi-task training (c), graphs remain confined to fixed task roles, and the same graph is not reused across functional contexts. Our interleaved role-based paradigm (d) exposes the *same* graph  $g \in \mathcal{G}_S$  to both structure-generation and structure-understanding roles, creating cross-role supervision. This role switching induces structural consistency and supports reusable graph representations across tasks and modalities.

modalities, with lightweight task-specific heads applied for different tasks (Wei et al., 2024; Zhu et al., 2025). Although graphs may implicitly arise in the shared model, they function primarily as task-internal intermediates rather than as persistent representations reused across tasks. As illustrated in Figure 3(c), graphs generated or used in one task do not typically participate in other task roles or learning contexts. Consequently, even when tasks operate in a common graph state space, their usage of graphs remains largely isolated, resulting in limited cross-role interaction.

To enable graphs to function as persistent intermediate representations across functional contexts, training must explicitly organize how they are reused under different task types. Interleaved generation-understanding training pipeline provides this organization. We model training as a sequence of *task-role instantiations* over unified graph states. Let  $\mathcal{T} = \{T_1, \dots, T_K\}$  denote a set of tasks under different modalities, and  $\mathcal{G}_S$  denotes the unified graph state space. Each task  $T_i$  is associated with a role function

$$\rho_i : \mathcal{G}_S \rightarrow \{\text{GENERATE}, \text{UNDERSTAND}\}, \quad (1)$$

where GENERATE corresponds to tasks that construct or refine the graph structure (e.g., scene graph generation, event graph extraction), and UNDERSTAND corresponds to tasks that operate on graph structure for reasoning, prediction, or

evaluation (e.g., graph algorithm).

Next, training is organized as a sequence  $\{(T_{i_t}, \rho_{i_t})\}_{t=1}^N$ , in which graphs produced under generation tasks may be reused as inputs under subsequent understanding tasks. To make the input-output flow explicit, we view each task  $T_i$  as an operator acting on graphs and, optionally, modality inputs. Let  $\mathcal{X}_i$  denote the modality-specific input space associated with  $T_i$ , and let  $\mathcal{Y}_i$  denote its task-specific output space. Each task induces a mapping

$$T_i : (\mathcal{X}_i, \mathcal{G}_S) \rightarrow (\mathcal{G}_S, \mathcal{Y}_i). \quad (2)$$

When  $\rho_i = \text{GENERATE}$ , the task produces or refines a graph:

$$G^{(t)} = T_i(x_i, G^{(t-1)}), \quad G^{(t)} \in \mathcal{G}_S. \quad (3)$$

When  $\rho_i = \text{UNDERSTAND}$ , the task treats the graph as an intermediate representation and produces predictions or supervision signals:

$$y_i^{(t)} = T_i(x_i, G^{(t)}), \quad y_i^{(t)} \in \mathcal{Y}_i. \quad (4)$$

Interleaving therefore induces a trajectory of a graph.  $G^{(0)} \rightarrow G^{(1)} \rightarrow \dots \rightarrow G^{(N)}$ , where graphs serve as persistent intermediate representations that evolve across successive generations and understanding tasks rather than

being reconstructed independently and discarded in each task, as illustrated in Figure 3(d).

From a representation-centric perspective, interleaving alters the supervision received by graphs rather than modifying individual task objectives. In task-isolated training, a graph is optimized under a single task type and only needs to satisfy constraints induced by that usage context. Under interleaved generation–understanding training, the same graph must remain usable across multiple task types. Graphs that support one type but are structurally incompatible with others receive inconsistent supervision and are gradually disfavored. This bias toward structurally coherent graphs emerges from the training organization itself, rather than from explicit regularization or parameter-level coupling.

### 3. Experiments

This section examines whether organizing learning around reusable intermediate graph leads to consistent improvements across heterogeneous learning settings mediated by graph structure. We study this question by contrasting G-Substrate with task-isolated training and naive multi-task learning, and by conducting controlled analyses that disentangle the roles of structural alignment and cross-role reuse of graph. We additionally assess how a unified, substrate-oriented framework compares to representative task-specific models under standard evaluation protocols.

#### 3.1. Learning Settings and Tasks

We evaluate the framework on four representative learning settings spanning domains and modalities. For each task, we describe its objective, model inputs and outputs, datasets, evaluation metrics, and task-specific baselines.

**Graph Algorithmic Reasoning (GAR).** This task predicts the outputs of classical graph algorithms from an input attributed graph. The model takes an attributed graph as input and outputs the answer to a graph algorithmic query. We consider connectivity (CT), cycle detection (CD), shortest path (SP), and bipartite matching (BM). We follow the datasets and evaluation settings in prior work (Wei et al., 2024; Wang et al., 2024b), and report accuracy as the evaluation metric. We compare against representative task-specific models for graph algorithmic reasoning, including GITA (Wei et al., 2024) and GraphWiz (Chen et al., 2024b).

**Molecular Graph Description (MGD).** This task requires generating a natural-language description of a molecule from its structural representation. The model takes a molecular graph (atoms and bonds), optionally accompanied by its SMILES string, as input and outputs a textual description of molecular properties or functionality. We use the Mol-Instructions dataset (Fang et al., 2024), and evaluate using BLEU-4 and ROUGE-L. We compare against the task-specific baseline Mol-LLaMA (Kim et al., 2025).

**Scene Graph Generation (SGG).** This task requires pre-

dicting a scene graph of objects and relations from an input image. The model takes an image as input and outputs a structured graph whose nodes correspond to objects and whose edges represent pairwise relations. Evaluation is conducted on Visual Genome (Krishna et al., 2017) under the PCIs and SGCLs protocols, reporting R@50 and mR@50, with PCIs R@50 as the primary metric. As ground-truth bounding boxes are unavailable in our setting, we follow the data processing protocol of (Li et al., 2024a). We compare against the task-specific baseline PGSG (Li et al., 2024a).

**Event Relation Extraction (ERE).** This task constructs event-relation graphs from text, capturing temporal, causal, or subevent structures among events. The model takes raw text as input and outputs a structured graph whose nodes correspond to events and whose edges encode typed relations. We evaluate on MAVEN-subevent (MA-S), MAVEN-temporal (MA-T), MAVEN-causal (MA-C) (Wang et al., 2022) and HiEvent (HiE) (Glavas et al., 2014), reporting precision, recall, and F1 score. We compare against task-specific baselines ProtoEM (Hu et al., 2023) and LLMERE (Hu et al., 2025e).

#### 3.2. Training Paradigms

We compare learning settings that differ along two orthogonal axes: (1) the representation of graph (task-specific vs. unified structural schema), and (2) the training organization (task-isolated, jointly multi-task, or with interleaved role-based training). This leads to six paradigms. **Naive single-task (NST)** and **Unified single-task (UST)** train each task in isolation, differing only in whether graph uses native formats or the unified schema. **Naive multi-task (NMT)** and **Unified multi-task (UMT)** jointly train all tasks, again differing in representation format but without exposing the same graph to multiple functional roles. **Naive multi-task + interleave (NMT-I)** introduces role-based interleaving on top of naive task-specific representations, allowing the graph to be reused under different task roles without structural alignment. **G-Substrate (Unified + interleave, G-Sub)** combines the unified schema with interleaved role-based training. Together, these paradigms disentangle the effects of structural alignment and cross-role reuse. Detailed definitions are given in Appendix D. All methods share the same backbone model and optimization settings. For multi-task settings, no additional task-specific fine-tuning after training or test-time adaptation is applied; each model is trained once under its corresponding paradigm and evaluated directly. Unless otherwise specified, experiments use the Qwen3-VL-2B-Instruct model (Team, 2025) as the backbone. Detailed training configurations are provided in Appendix E.

#### 3.3. Main Results

Table 2 summarizes the main results across heterogeneous learning settings. Despite using a single unified model rather

**Table 2. Main results across modalities, domains, and tasks.** Best results are in **bold**; second-best are underlined. GAR (Graph Algorithmic Reasoning) is evaluated using **accuracy** for each task (CT: Connectivity, CD: Cycle Detection, SP: Shortest Path, BM: Bipartite Matching). MGD (Molecular Graph Description) is evaluated using **BLEU-4** and **ROUGE-L**. SGG (Scene Graph Generation) reports **PCIs R@50**. ERE (Event Relation Extraction) reports **F1 scores** on MAVEN-S, MAVEN-T, MAVEN-C, and HiEvent.

Method	GAR				MGD		SGG		ERE			
	CT	CD	SP	BM	BLEU-4	ROUGE-L	PCIs	MA-S	MA-T	MA-C	HiE	
<b>Task-Specific Training</b>												
GITA (Wei et al., 2024)	98.17	<b>98.07</b>	39.15	93.19	—	—	—	—	—	—	—	—
G-Wiz (Chen et al., 2024b)	97.74	95.46	41.46	92.15	—	—	—	—	—	—	—	—
M-LLama (Kim et al., 2025)	—	—	—	—	<u>50.74</u>	67.02	—	—	—	—	—	—
PGSG (Li et al., 2024a)	—	—	—	—	—	—	<b>26.9</b>	—	—	—	—	—
ProtoEM (Hu et al., 2023)	—	—	—	—	—	—	—	<u>53.80</u>	31.80	27.90	20.43	
LLMERE (Hu et al., 2025e)	—	—	—	—	—	—	—	<b>54.30</b>	35.60	27.90	<u>22.90</u>	
Naive single-task	<u>99.44</u>	92.18	38.27	92.05	48.59	66.65	23.74	39.65	<u>41.60</u>	27.70	17.10	
Unified single-task	97.80	94.70	37.14	85.98	47.35	65.64	22.43	45.45	<u>33.29</u>	30.22	14.28	
<b>Multi-Task Training</b>												
Naive multi-task	<b>99.71</b>	94.72	41.27	92.21	48.11	66.11	24.68	36.87	39.14	37.02	18.78	
Unified multi-task	98.09	96.19	<u>45.02</u>	<u>94.23</u>	49.99	<u>67.36</u>	25.36	51.89	40.05	<u>40.75</u>	19.37	
Naive multi-task + interleave	98.27	93.86	43.83	91.92	48.63	64.98	24.02	45.74	38.86	37.99	21.36	
<b>G-Substrate (Ours)</b>	98.41	<u>96.97</u>	<b>48.59</b>	<b>94.54</b>	<b>51.53</b>	<b>68.47</b>	<u>25.38</u>	52.20	<b>42.68</b>	<b>40.91</b>	<b>25.15</b>	

than domain-specialized architectures, G-Substrate achieves performance that is competitive with or superior to these task-specific systems in most settings. These results indicate that organizing learning around a shared relational substrate does not sacrifice domain-specific capability and can match or exceed specialized pipelines.

We next analyze the effect of different training paradigms. G-Substrate outperforms both task-isolated training and naive multi-task learning on most metrics. The improvements are more pronounced in settings with stronger structural demands, suggesting that the gains are tied to structural reasoning rather than uniform scaling effects. These patterns are consistent with the intended mechanism of G-Substrate. Task-isolated training restricts graphs to a single functional context, while naive multi-task learning, despite parameter sharing, does not require the same graph to remain usable across roles. By contrast, G-Substrate combines structural alignment with interleaved generation-understanding training, encouraging graphs to remain valid under multiple roles. This cross-role pressure biases representations toward relational regularities rather than task-specific shortcuts, aligning with the observed performance trends. Detailed results are provided in Appendix F.

### 3.4. Analysis

We conduct controlled studies to analyze the mechanisms underlying G-Substrate, isolating representation and training-organization factors while keeping the backbone, data, and training budget fixed. Specifically, we examine: (i) the interaction between structural alignment and role-based training, (ii) the effect of schema realization, (iii) cross-domain structural transfer, (iv) the contribution of different

cross-role training instantiations, (v) the role of structural correctness of the reused graph, and (vi) the impact of the proportion of role-based interleaving.

#### 3.4.1. UNIFIED STRATEGY ANALYSIS

**Schema–Training Interaction.** We examine whether the effect of unified representations arises from the structural schema itself or from its interaction with role-based training. Table 2 shows that the *Unified Single-Task* setting does not outperform the *Naive Single-Task* baseline and often performs worse under task-isolated training. In contrast, unified representations improve performance when the same graph is exposed to multiple functional roles during training. This indicates that the schema primarily establishes structural compatibility, whose benefits emerge only when the graph is reused across roles rather than optimized in isolation.

**Effect of Schema Realization.** We compare different realizations of the unified schema, including natural-language descriptions, XML-style serializations, and the schema representation used in G-Substrate, all encoding an identical graph under the same role-based training setting. Table 3 shows that although alternative serializations permit basic transfer, their performance is generally less stable. XML-style formats, in particular, tend to underperform, likely because strict formatting encourages attention to surface structure rather than underlying relational semantics. The proposed schema realization provides more reliable performance, indicating that effective structural reuse depends not only on schema unification, but also on how relational structure is expressed when the graph is exercised under multiple functional roles during training.

**Cross-domain Structural Transfer.** To assess cross-

**Table 3. Effect of Schema Realization.** Performance comparison of different schema realizations under identical multi-task training conditions. The best-performing method is shown in **bold**.

Method	GAR				MGD		PCIs	SGG				ERE			
	CT	CD	SP	BM	BLEU-4	ROUGE-L		MA-S	MA-T	MA-C	HiE				
Natural Language	97.15	94.20	44.80	92.75	49.20	66.80	24.10	50.80	40.95	39.20	23.90				
XML-style	94.80	92.30	40.10	88.40	44.60	60.50	23.65	46.30	36.40	34.70	20.80				
<b>Ours</b>	<b>98.41</b>	<b>96.97</b>	<b>48.59</b>	<b>94.54</b>	<b>51.53</b>	<b>68.47</b>	<b>25.38</b>	<b>52.20</b>	<b>42.68</b>	<b>40.91</b>	<b>25.15</b>				

**Table 4. Cross-domain structural transfer from event graphs to scene graph generation.** Models are evaluated on scene graph generation (PCIs R@50).  $\Delta$  denotes the absolute performance change relative to the Base model. No scene-graph data is used during source-domain training.

Pretraining Setting	SGG	$\Delta$
Base (no domain training)	19.10	–
Event-only (unified schema)	21.47	+2.37

domain reuse of graph structure, we transfer from event-centric text graphs to scene graph generation. Table 4 reports performance relative to a base model without domain-specific pretraining. Training on event graphs alone improves scene graph generation despite the absence of target-domain supervision. This suggests that learning organized around an explicit graph structure can capture structural regularities that transfer across domains, rather than being fully tied to a single task or modality.

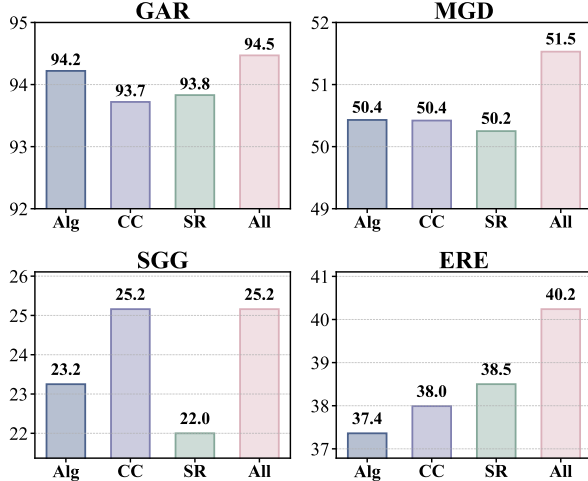


**Figure 4. Contribution of different interleaving supervision types.** Metrics are averaged accuracy for GAR, BLEU-4 for MGD, PCIs R@50 for SGG, and macro-averaged F1 for ERE.

### 3.4.2. INTERLEAVING STRATEGY ANALYSIS

**Cross-task Influence.** To analyze how different cross-role training instantiations contribute to learning, we vary the composition of role-based exposure sources while keeping the overall training budget fixed. Specifically, we consider three types of role-based supervision: graph algorithmic (Alg), consistency checking (CC), subgraph retrieval (SR), and their combination. Alg requires structural reasoning

over graphs (e.g., connectivity), encouraging preservation of global structure. CC presents the original modality input (text or image) together with a candidate graph and predicts whether they are consistent; negative examples are constructed by perturbing the graph, promoting alignment between graph structure and underlying inputs. SR operates on scene and event graphs, requiring the model to extract or recognize meaningful subgraphs, encouraging localized structural reasoning and compositional reuse. Figure 4 shows the resulting performance changes relative to unified multi-task training without role-based interleaving. Gains are not uniform, but relate systematically to the domain structural characteristics: highly constrained graph domains show smaller improvements, whereas more weakly constrained domains benefit more from additional cross-role structural exposure. Effects also depend on the supervision type, with consistency checking and subgraph retrieval often yield stronger gains, particularly when supervision is grounded in the same evidence modality. These trends indicate that role-based interleaving reshapes representation-level structural pressures on the persistent graph rather than uniformly enhancing all tasks.

**Structural Correctness of Reused Graphs.** We test whether the gains from role-based interleaving depend on structural coherence rather than superficial serialization. Persistent graphs reused under multiple functional roles are replaced with structurally incorrect variants that preserve node and edge labels but disrupt relational connectivity. As shown in Figure 5, performance gains largely disappear when structurally incorrect graphs are used. This contrast indicates that cross-role training is sensitive to the relational organization of the graph, and that malformed structures introduce misleading signals at the representation level.

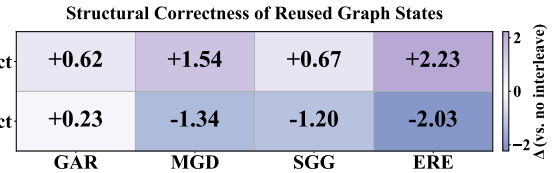


**Figure 5. Effect of structural correctness of reused graph.** Performance change ( $\Delta$  vs. unified multi-task) for structurally correct and incorrect graphs. Metrics are averaged accuracy for GAR, BLEU-4 for MGD, PCIs R@50 for SGG, and macro-averaged F1 for ERE.

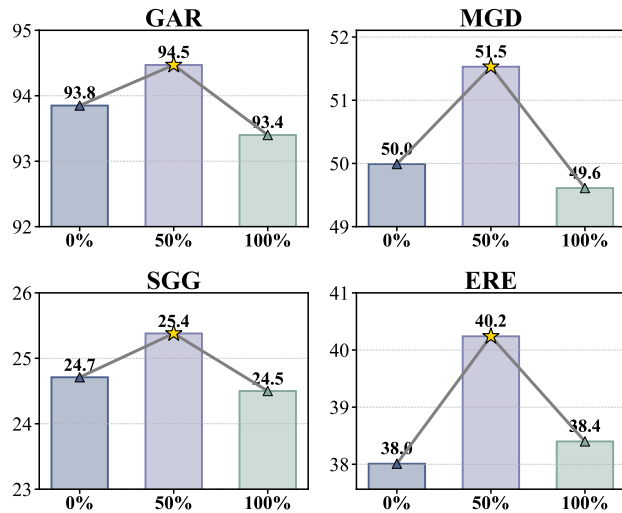


Figure 6. Effect of interleaving proportion. Performance of each domain as the ratio of newly introduced interleaved training instances to the unified multi-task data increases (0, 50%, 100%). Metrics are averaged accuracy for GAR, BLEU-4 for MGD, PCIs R@50 for SGG, and averaged F1 for ERE.

**Effect of Role-based Interleaving Proportion.** Finally, we analyze how the relative proportion of role-based exposure affects performance. As shown in Figure 6, we vary the ratio of training instances in which persistent graphs are exercised under multiple functional roles to those drawn from standard unified multi-task training. Moderate levels of cross-role exposure consistently yield the greatest improvements, whereas excessive role-based interleaving degrades performance by weakening task-specific optimization signals. This trend indicates that effective role-based training requires balancing structural exposure of the graph across roles with sufficient task-focused learning. Together, these results suggest that role-based interleaving operates as a controlled mechanism for representation reuse rather than as unrestricted task mixing. Results with an alternative backbone show similar trends (Appendix G), suggesting the gains arise from representation design and training organization rather than the backbone.

#### 4. Related Work

**Graphs as a ubiquitous but task-bound tool.** Graph-structured representations have become a standard modeling device across diverse domains (Wang et al., 2025b; Hu et al., 2025c; Chen et al., 2024b; Wang et al., 2024b; 2023; Yuan et al., 2025b; Zhang et al., 2019; Ju et al., 2022). Some works focus on inducing graphs from perceptual or linguistic inputs, such as scene graph generation from images and event graph extraction from text (Chen et al., 2024d; Li et al., 2024a; Liu et al., 2025; Xu et al., 2025c; Zhang et al., 2022). Other works adopt graph-conditioned reasoning paradigms, including molecular understanding and structured semantic prediction (Kim et al., 2025; Liu et al., 2024c; Park et al., 2024; Guo et al., 2021; 2020).

Despite the recurrence of similar structural patterns across domains, existing systems almost universally treat graph structure as a *task-scoped artifact*: graphs are constructed to satisfy a particular objective, optimized within a single task pipeline, and discarded thereafter. Consequently, graph representations do not function as reusable state across heterogeneous learning contexts, and structural regularities are repeatedly rediscovered rather than accumulated.

**Multi-task learning.** Multi-task learning (MTL) has long been studied as a paradigm for coordinating learning across related tasks (Ruder, 2017; Akhtar et al., 2020; Yuan et al., 2025a; Zhang & Yang, 2022; Sanh et al., 2021). More recently, large language models and vision–language models have significantly extended this paradigm by leveraging large-scale pretraining, unified architectures, and instruction-based or prompt-based task formulations to support broad task generalization (Kong et al., 2025; Sun et al., 2025; Wang et al., 2024e; He et al., 2024; Liu et al., 2024b; Wang et al., 2025g; Lu et al., 2019; Tan & Bansal, 2019; Chen et al., 2020). Despite these advances, most existing LLM- and VLM-based multi-task frameworks rely on implicit knowledge storage in model parameters (Zhang et al., 2026; Khashabi et al., 2020; Mishra et al., 2022), enabled by shared objectives and architectures, rather than on explicitly modeling and reusing structured representations across tasks. Consequently, while effective at multi-task prediction, they fall short of exploiting recurring graph structures across tasks as an explicit and reusable source of inductive bias.

**Graph as a unified substrate across modalities.** We argue that existing limitations stem from representation design. We therefore treat graph structure as a persistent intermediate state shared across domains and modalities, instead of a task-bound interface, enabling structural knowledge to accumulate and transfer across learning tasks. Appendix H provides further discussion.

#### 5. Conclusion

Graph structures arise across diverse domains, modalities, and tasks, but are typically optimized in isolated learning contexts and discarded thereafter, preventing them from serving as persistent intermediate representations. We argue that this limitation stems from a task-centric organization of learning that treats intermediate structure as disposable rather than reusable. To address this issue, we introduce G-Substrate, a framework that enables representation reuse through two complementary mechanisms: a unified structural space that ensures cross-task compatibility, and interleaved role-based training that exposes the same graph to multiple functional roles. Experiments across heterogeneous settings consistently show that both structural alignment and cross-role reuse contribute to performance, while their combination yields the most consistent gains. Together, these findings indicate that persistent graph representations are a key driver of structural reuse and improved performance across diverse learning contexts.

## Impact Statement

We propose a representation-centric framework that treats graph structure as a reusable intermediate substrate across tasks and modalities, enabling learning systems to accumulate and reuse relational structure rather than repeatedly reconstructing it in isolation. By improving cross-task and cross-domain structural reuse, this approach has the potential to increase data efficiency, reduce redundant supervision, and support more generalizable AI systems that operate over structured information such as events, scenes, molecules, and algorithmic graphs.

Potential positive societal impacts include improved scientific modeling (e.g., molecular understanding), better structured information extraction from text, and more robust reasoning systems that can integrate heterogeneous data sources. However, as with other foundation-style learning frameworks, the method may inherit biases present in underlying datasets, including linguistic, visual, or scientific knowledge biases. Because graph states abstract relational structure, systematic biases in how entities or relations are represented (e.g., in event corpora or visual datasets) may propagate across tasks when representations are reused.

The framework does not itself bring about new surveillance, personal data gathering, or autonomous decision making, but it could be integrated into bigger systems that already do. Responsible deployment therefore depends on consideration of the dataset composition, transparent graph construction processes, and evaluation across domains to mitigate the risk that structural reuse will exacerbate domain-specific biases. Further research targeting balancing heterogeneous supervision and controlling cross-domain transfer will be critical to controlling unintended results from representation reuse at scale.

**Limitations and Future Work.** We do not explicitly study how the composition of modalities, domains, or role types influences representation formation, and the optimal balance among structure-producing, structure-consuming, and algorithmic roles remains open. Future work may explore principled strategies for balancing heterogeneous role-based supervision and for extending this representation-centric principle to other forms of structured intermediate representations beyond graphs.

## References

Akhtar, M. S., Chauhan, D. S., and Ekbal, A. A deep multi-task contextual attention framework for multi-modal affect analysis. *TKDD*, 2020.

Battaglia, P. W., Hamrick, J. B., Bapst, V., Sanchez-Gonzalez, A., Zambaldi, V. F., Malinowski, M., Tacchetti, A., Raposo, D., Santoro, A., Faulkner, R., Gülcühre, Ç., Song, H. F., Ballard, A. J., Gilmer, J., Dahl, G. E., Vaswani, A., Allen, K. R., Nash, C., Langston, V., Dyer, C., Heess, N., Wierstra, D., Kohli, P., Botvinick, M. M., Vinyals, O., Li, Y., and Pascanu, R. Relational inductive biases, deep learning, and graph networks. *CoRR*, 2018.

Bi, J., Wang, Y., Chen, H., Xiao, X., Hecker, A., Tresp, V., and Ma, Y. LLaVA steering: Visual instruction tuning with 500x fewer parameters through modality linear representation-steering. In *ACL*, 2025a.

Bi, J., Wang, Y., Yan, D., Aniri, Huang, W., Jin, Z., Ma, X., Hecker, A., Ye, M., Xiao, X., Schuetze, H., Tresp, V., and Ma, Y. Prism: Self-pruning intrinsic selection method for training-free multimodal data selection, 2025b.

Bi, J., Yan, D., Wang, Y., Huang, W., Chen, H., Wan, G., Ye, M., Xiao, X., Schuetze, H., Tresp, V., et al. Cot-kinetics: A theoretical modeling assessing lrm reasoning process. *CoRR*, 2025c.

Chai, Z., Zhang, T., Wu, L., Han, K., Hu, X., Huang, X., and Yang, Y. Graphilm: Boosting graph reasoning ability of large language model. *TBD*, 2025.

Chen, M., Peng, B., Zhang, Y., and Lu, C. CELLO: causal evaluation of large vision-language models. In *ENMLP*, 2024a.

Chen, N., Li, Y., Tang, J., and Li, J. Graphwiz: An instruction-following language model for graph computational problems. In *SIGKDD*, 2024b.

Chen, R., Zhao, T., Jaiswal, A. K., Shah, N., and Wang, Z. Lлага: Large language and graph assistant. In *ICML*, 2024c.

Chen, X., Lu, J., Kim, M., Zhang, D., Tang, J., Piché, A., Gontier, N., Bengio, Y., and Kamalloo, E. Self-evolving curriculum for LLM reasoning. *CoRR*, 2025a.

Chen, Y.-C., Li, L., Yu, L., El Kholy, A., Ahmed, F., Gan, Z., Cheng, Y., and Liu, J. Uniter: Universal image-text representation learning. In *ECCV*, 2020.

Chen, Z., Wu, J., Lei, Z., Zhang, Z., and Chen, C. W. Expanding scene graph boundaries: Fully open-vocabulary scene graph generation via visual-concept alignment and retention. In *ECCV*, 2024d.

Chen, Z., Wu, J., Lei, Z., and Chen, C. W. From data to modeling: Fully open-vocabulary scene graph generation. *CoRR*, 2025b.

Ding, X., Ping, K., Çarik, B., and Rho, E. H. R. A multi-level benchmark for causal language understanding in social media discourse. *CoRR*, 2025.

Dutta, A., Mehrab, K. S., Sawhney, M., Neog, A., Khurana, M., Fatemi, S., Pradhan, A., Maruf, M., Lourentzou, I., Daw, A., et al. Open world scene graph generation using vision language models. *CoRR*, 2025.

Elshawy, A., Li, M., Navab, N., and Busam, B. PRISM-0: A predicate-rich scene graph generation framework for zero-shot open-vocabulary tasks. *CoRR*, 2025.

Fang, Y., Liang, X., Zhang, N., Liu, K., Huang, R., Chen, Z., Fan, X., and Chen, H. Mol-instructions: A large-scale biomolecular instruction dataset for large language models. In *ICLR*, 2024.

Glavas, G., Snajder, J., Moens, M., and Kordjamshidi, P. Hieve: A corpus for extracting event hierarchies from news stories. In *LREC*, 2014.

Gong, Z., Yu, H., Liao, C., Liu, B., Chen, C., and Li, J. Coba: Convergence balancer for multitask finetuning of large language models. In *EMNLP*, 2024.

Guo, Z., Yu, W., Zhang, C., Jiang, M., and Chawla, N. V. Graseq: graph and sequence fusion learning for molecular property prediction. In *CIKM*, 2020.

Guo, Z., Zhang, C., Yu, W., Herr, J., Wiest, O., Jiang, M., and Chawla, N. V. Few-shot graph learning for molecular property prediction. In *WWW*, 2021.

Hamilton, W. L., Ying, Z., and Leskovec, J. Inductive representation learning on large graphs. In *NeurIPS*, 2017.

He, X., Tian, Y., Sun, Y., Chawla, N. V., Laurent, T., LeCun, Y., Bresson, X., and Hooi, B. G-retriever: Retrieval-augmented generation for textual graph understanding and question answering. In *NeurIPS*, 2024.

Hu, X., Qin, K., Duan, G., Li, M., Li, Y.-F., and He, T. Spade: spatial-aware denoising network for open-vocabulary panoptic scene graph generation with long- and local-range context reasoning. In *ICCV*, 2025a.

Hu, Y., Ding, C., Sun, C., Huang, S., and Xu, X. Bilateral collaboration with large vision-language models for open vocabulary human-object interaction detection. *CVPR*, 2025b.

Hu, Y., Huang, X., Wei, Z., Liu, Y., and Hong, C. Rethinking and benchmarking large language models for graph reasoning. *CoRR*, 2025c.

Hu, Y., Zhang, F., Wei, R., and Gao, J. Learning semantic-unified cross-modal representations for open-vocabulary video scene graph generation. *Multim. Syst.*, 2025d.

Hu, Z., Li, Z., Xu, D., Bai, L., Jin, C., Jin, X., Guo, J., and Cheng, X. Protoem: A prototype-enhanced matching framework for event relation extraction. *CoRR*, 2023.

Hu, Z., Li, Y., Chen, Z., Wang, J., Liu, H., Lee, K., and Ding, K. Let's ask GNN: empowering large language model for graph in-context learning. In *EMNLP*, 2024.

Hu, Z., Li, Z., Jin, X., Bai, L., Guo, J., and Cheng, X. Large language model-based event relation extraction with rationales. In *COLING*, 2025e.

Jiang, X., Qiu, R., Xu, Y., Zhang, W., Zhu, Y., Zhang, R., Fang, Y., Xu, C., Zhao, J., and Wang, Y. Ragraph: A general retrieval-augmented graph learning framework. In *NeurIPS*, 2024.

Jin, C., Guo, S., Zhou, S., and Guan, J. Effective and explainable molecular property prediction by chain-of-thought enabled large language models and multi-modal molecular information fusion. *Journal of Chemical Information and Modeling*, 2025.

Ju, M., Zhao, T., Wen, Q., Yu, W., Shah, N., Ye, Y., and Zhang, C. Multi-task self-supervised graph neural networks enable stronger task generalization. In *ICLR*.

Ju, M., Yu, W., Zhao, T., Zhang, C., and Ye, Y. Grape: Knowledge graph enhanced passage reader for open-domain question answering. In *EMNLP*, 2022.

Khashabi, D., Min, S., Khot, T., Sabharwal, A., Tafjord, O., Clark, P., and Hajishirzi, H. Unifiedqa: Crossing format boundaries with a single qa system. *CoRR*, 2020.

Kim, D., Lee, W., and Hwang, S. J. Mol-llama: Towards general understanding of molecules in large molecular language model. *CoRR*, 2025.

Kong, L., Feng, J., Liu, H., Huang, C., Huang, J., Chen, Y., and Zhang, M. GOFA: A generative one-for-all model for joint graph language modeling. In *ICLR*, 2025.

Kong, Z. and Zhang, H. Opensgen: Fine-grained relation-aware prompt for open-vocabulary scene graph generation. In Zhang, Z. M., Ricci, E., Yan, Y., Nie, L., Oria, V., and Ballan, L. (eds.), *ICMR*, 2025.

Krishna, R., Zhu, Y., Groth, O., Johnson, J., Hata, K., Kravitz, J., Chen, S., Kalantidis, Y., Li, L., Shamma, D. A., Bernstein, M. S., and Fei-Fei, L. Visual genome: Connecting language and vision using crowdsourced dense image annotations. *IJCV*, 2017.

Lafferty, J. D., McCallum, A., and Pereira, F. C. N. Conditional random fields: Probabilistic models for segmenting and labeling sequence data. In *ICML*, 2001.

Leng, Y. and Xiong, D. Towards understanding multi-task learning (generalization) of llms via detecting and exploring task-specific neurons. In *COLING*, 2025.

Li, B., Han, X., Liu, J., Ding, Y., Jing, L., Zhang, Z., Li, J., Du, X., Li, F., Zhang, M., et al. Event extraction in large language model. *CoRR*, 2025a.

Li, J., Li, J., and Zhang, C. Instance-aware graph prompt learning. *TMLR*.

Li, J., Wu, R., Zhu, Y., Zhang, H., Chen, L., and Zheng, Z. Are large language models in-context graph learners? *CoRR*, 2025b.

Li, L., Zhang, C., Zhang, D., Sun, C., Li, C., and Chen, L. Taking A closer look at interacting objects: Interaction-aware open vocabulary scene graph generation. *CoRR*, 2025c.

Li, R., Zhang, S., Lin, D., Chen, K., and He, X. From pixels to graphs: Open-vocabulary scene graph generation with vision-language models. In *CVPR*, 2024a.

Li, Y., Hu, B., Shi, H., Wang, W., Wang, L., and Zhang, M. Visiongraph: Leveraging large multimodal models for graph theory problems in visual context. In *ICML*, 2024b.

Lin, T., Yan, P., Song, K., Jiang, Z., Kang, Y., Lin, J., Yuan, W., Cao, J., Sun, C., and Liu, X. Langgfm: A large language model alone can be a powerful graph foundation model. *CoRR*, 2024.

Liu, B., Chen, C., Gong, Z., Liao, C., Wang, H., Lei, Z., Liang, M., Chen, D., Shen, M., Zhou, H., Jiang, W., Yu, H., and Li, J. Mftcoder: Boosting code llms with multitask fine-tuning. In *SIGKDD*, 2024a.

Liu, H., Feng, J., Kong, L., Liang, N., Tao, D., Chen, Y., and Zhang, M. One for all: Towards training one graph model for all classification tasks. In *ICLR*, 2024b.

Liu, J., Yang, C., Lu, Z., Chen, J., Li, Y., Zhang, M., Bai, T., Fang, Y., Sun, L., Yu, P. S., and Shi, C. Towards graph foundation models: A survey and beyond. *CoRR*, 2023.

Liu, P., Ren, Y., Tao, J., and Ren, Z. Git-mol: A multi-modal large language model for molecular science with graph, image, and text. *Comput. Biol. Medicine*, 2024c.

Liu, T., Li, R., Wang, C., and He, X. Relation-aware hierarchical prompt for open-vocabulary scene graph generation. In *AAAI*, 2025.

Liu, Z. and Wang, C. Terdy: Temporal relation dynamics through frequency decomposition for temporal knowledge graph completion. In *ACL*, 2025.

Liu, Z., He, X., Tian, Y., and Chawla, N. V. Can we soft prompt llms for graph learning tasks? In *WWW*, 2024d.

Lu, J., Batra, D., Parikh, D., and Lee, S. Vilbert: Pretraining task-agnostic visiolinguistic representations for vision-and-language tasks. *NeurIPS*, 2019.

Luo, H., Meng, X., Wang, S., Zhao, T., Wang, F., Cao, H., and Zhang, Y. Enhance graph alignment for large language models. *CoRR*, 2024a.

Luo, Y., Zhang, J., Fan, S., Yang, K., Hong, M., Wu, Y., Qiao, M., and Nie, Z. Biomedgpt: An open multimodal large language model for biomedicine. *IEEE JBHI*, 2024b.

Ma, T., Qian, Y., Wang, Z., Zhang, Z., Zhang, C., and Ye, Y. Llm-empowered class imbalanced graph prompt learning for online drug trafficking detection. In *ACL*, 2025.

Min, Y., Yang, M., Zhang, J., Wang, Y., Wu, A., and Deng, C. Vision-language interactive relation mining for open-vocabulary scene graph generation. In *ICCV*, 2025.

Mishra, S., Khashabi, D., Baral, C., and Hajishirzi, H. Cross-task generalization via natural language crowdsourcing instructions. In *ACL*, 2022.

Pan, D., Fu, Z., Wang, J., Han, X., Zhu, Y., and Zhao, X. Contextual attention modulation: Towards efficient multi-task adaptation in large language models. In *CIKM*, 2025.

Park, J., Bae, M., Ko, D., and Kim, H. J. Llamo: Large language model-based molecular graph assistant. In *NeurIPS*, 2024.

Ruder, S. An overview of multi-task learning in deep neural networks. *CoRR*, 2017.

Sanh, V., Webson, A., Raffel, C., Bach, S. H., Sutawika, L., Alyafeai, Z., Chaffin, A., Stiegler, A., Scao, T. L., Raja, A., et al. Multitask prompted training enables zero-shot task generalization. *CoRR*, 2021.

Sartori, C. C., Blum, C., and Bistaffa, F. Visgraphvar: A benchmark generator for assessing variability in graph analysis using large vision-language models. *Access*, 2025.

Standley, T., Zamir, A., Chen, D., Guibas, L. J., Malik, J., and Savarese, S. Which tasks should be learned together in multi-task learning? In *ICML*, 2020.

Sun, Y., Ma, Z., Fang, Y., Ma, J., and Tan, Q. Graphicl: Unlocking graph learning potential in llms through structured prompt design. In *NAACL*, 2025.

Tan, H. and Bansal, M. Lxmert: Learning cross-modality encoder representations from transformers. *CoRR*, 2019.

Tanев, H., Stefanovitch, N., Harmatha, T., and Sousa, D. F. Exploring the performance of large language models for event detection and extraction in the health domain. In *RANLP*, 2025.

Tang, J., Yang, Y., Wei, W., Shi, L., Su, L., Cheng, S., Yin, D., and Huang, C. Graphgpt: Graph instruction tuning for large language models. In *SIGIR*, 2024a.

Tang, J., Zhang, Q., Li, Y., Chen, N., and Li, J. Grapharena: Evaluating and exploring large language models on graph computation. *CoRR*, 2024b.

Tao, Z., Jin, Z., Zhang, Y., Chen, X., Zhao, H., Li, J., Liang, B., Tao, C., Liu, Q., and Wong, K.-F. A comprehensive evaluation on event reasoning of large language models. In *AAAI*, 2025.

Team, Q. Qwen3 technical report, 2025.

Thapaliya, S., Wang, Z., Li, J., Li, Z., Ye, Y., and Zhang, C. Semantic refinement with llms for graph representations. *arXiv preprint arXiv:2512.21106*, 2025.

Wang, D., Zuo, Y., Li, F., and Wu, J. Llms as zero-shot graph learners: Alignment of GNN representations with LLM token embeddings. In *NeurIPS*, 2024a.

Wang, H., Feng, S., He, T., Tan, Z., Han, X., and Tsvetkov, Y. Can language models solve graph problems in natural language? In *NeurIPS*, 2023.

Wang, J., Wu, J., Hou, Y., Liu, Y., Gao, M., and McAuley, J. J. Instructgraph: Boosting large language models via graph-centric instruction tuning and preference alignment. In *ACL*, 2024b.

Wang, R., Liang, S., Chen, Q., Zhang, J., and Qin, K. Graphtool-instruction: Revolutionizing graph reasoning in llms through decomposed subtask instruction. In *SIGKDD*, 2025a.

Wang, X., Chen, Y., Ding, N., Peng, H., Wang, Z., Lin, Y., Han, X., Hou, L., Li, J., Liu, Z., Li, P., and Zhou, J. MAVEN-ERE: A unified large-scale dataset for event coreference, temporal, causal, and subevent relation extraction. In *EMNLP*, 2022.

Wang, X., Zhou, Y., Chen, H., and Zhu, W. Curriculum learning: Theories, approaches, applications, tools, and future directions in the era of large language models. In *WWW*, 2024c.

Wang, Y., Liu, B., Tang, J., Chen, N., Li, Y., Zhang, Q., and Li, J. Graph-r1: Unleashing LLM reasoning with np-hard graph problems. *CoRR*, 2025b.

Wang, Y., Wu, X., Yang, S., and Luo, J. End-to-end open-vocabulary video visual relationship detection using multi-modal prompting. *TPAMI*, 2025c.

Wang, Z., Xia, L., Xjtu, W., and Du, X. Document-level causal relation extraction with knowledge-guided binary question answering. In *EMNLP*, 2024d.

Wang, Z., Zhang, Z., Chawla, N. V., Zhang, C., and Ye, Y. GFT: graph foundation model with transferable tree vocabulary. In *NeurIPS*, 2024e.

Wang, Z., Zhang, Z., Ma, T., Chawla, N. V., Zhang, C., and Ye, Y. Learning cross-task generalities across graphs via task-trees. *CoRR*, 2024f.

Wang, Z., Liu, S., Zhang, Z., Ma, T., Zhang, C., and Ye, Y. Can llms convert graphs to text-attributed graphs? In *NAACL*, 2025d.

Wang, Z., Liu, Z., Ma, T., Li, J., Zhang, Z., Fu, X., Li, Y., Yuan, Z., Song, W., Ma, Y., Zeng, Q., Chen, X., Zhao, J., Li, J., Jiang, M., Lio, P., Chawla, N. V., Zhang, C., and Ye, Y. Graph foundation models: A comprehensive survey. *CoRR*, 2025e.

Wang, Z., Zhang, Z., Ma, T., Chawla, N. V., Zhang, C., and Ye, Y. Beyond message passing: Neural graph pattern machine. In *ICML*, 2025f.

Wang, Z., Zhang, Z., Ma, T., Zhang, C., and Ye, Y. Generative graph pattern machine. In *NeurIPS*, 2025g.

Wei, Y., Fu, S., Jiang, W., Zhang, Z., Zeng, Z., Wu, Q., Kwok, J. T., and Zhang, Y. GITA: graph to visual and textual integration for vision-language graph reasoning. In *NeurIPS*, 2024.

Wu, S., Fei, H., and Chua, T.-S. Universal scene graph generation. In *CVPR*, 2025a.

Wu, W., Wang, C., Chen, L., Yin, M., Zhu, Y., Fu, K., Ye, J., Xiong, H., and Wang, Z. Structure-enhanced protein instruction tuning: Towards general-purpose protein understanding with llms. In *SIGKDD*, 2025b.

Xia, Y., Fu, F., Zhang, W., Jiang, J., and Cui, B. Efficient multi-task LLM quantization and serving for multiple lora adapters. In *NeurIPS*, 2024.

Xu, H., Jian, X., Zhao, X., Pang, W., Zhang, C., Wang, S., Zhang, Q., Monteiro, J., Sun, Q., and Yu, T. Graphomni: A comprehensive and extendable benchmark framework for large language models on graph-theoretic tasks. *CoRR*, 2025a.

Xu, J., Sun, M., Zhang, Z., and Zhou, J. Maqinstruct: Instruction-based unified event relation extraction. In *WWW*, 2025b.

Xu, M., Wu, M., Zhao, Y., Li, J. C. L., and Ou, W. Llava-spacesgg: Visual instruct tuning for open-vocabulary scene graph generation with enhanced spatial relations. In *WACV*, 2025c.

Yin, T., Zhang, X., Zhang, J., Huang, L., Zhang, Z., Zeng, Y., Xie, J., and Yan, M. Mora: On-the-fly molecule-aware low-rank adaptation framework for llm-based multi-modal molecular assistant. *CoRR*, 2025.

Yu, X., Zhou, C., Fang, Y., and Zhang, X. Multigprompt for multi-task pre-training and prompting on graphs. In *WWW*, 2024.

Yuan, Y., Li, Z., and Zhao, B. A survey of multimodal learning: Methods, applications, and future. *ACM Comput. Surv.*, 2025a.

Yuan, Z., Liu, M., Wang, H., and Qin, B. Gracore: Benchmarking graph comprehension and complex reasoning in large language models. In *COLING*, 2025b.

Zellers, R., Yatskar, M., Thomson, S., and Choi, Y. Neural motifs: Scene graph parsing with global context. In *CVPR*, 2018.

Zhang, C., Song, D., Huang, C., Swami, A., and Chawla, N. V. Heterogeneous graph neural network. In *KDD*, 2019.

Zhang, C., Huang, C., Li, Y., Zhang, X., Ye, Y., and Zhang, C. Look twice as much as you say: Scene graph contrastive learning for self-supervised image caption generation. In *CIKM*, 2022.

Zhang, J., You, J., Panda, A., and Goldstein, T. Lori: Reducing cross-task interference in multi-task low-rank adaptation. *CoRR*, 2025.

Zhang, M., Sun, M., Wang, P., Fan, S., Mo, Y., Xu, X., Liu, H., Yang, C., and Shi, C. Graphtranslator: Aligning graph model to large language model for open-ended tasks. In *WWW*, 2024a.

Zhang, Q., Hong, X., Tang, J., Chen, N., Li, Y., Li, W., Tang, J., and Li, J. Gcoder: Improving large language model for generalized graph problem solving. *CoRR*, 2024b.

Zhang, S., Dong, L., Li, X., Zhang, S., Sun, X., Wang, S., Li, J., Hu, R., Zhang, T., Wang, G., et al. Instruction tuning for large language models: A survey. *ACM Comput. Surv.*, 2026.

Zhang, Y. and Yang, Q. A survey on multi-task learning. *TKDE*, 2022.

Zhao, C., Su, X., He, M., Zhao, H., Fan, J., and Li, X. Collaborative knowledge fusion: A novel method for multi-task recommender systems via llms. *TKDE*, 2025a.

Zhao, J., Cheong, K. H., and Pedrycz, W. Bridging visualization and optimization: Multimodal large language models on graph-structured combinatorial optimization. *CoRR*, 2025b.

Zhao, J., Ning, W., Fei, Y., Feng, Y., and Li, L. GDLLM: A global distance-aware modeling approach based on large language models for event temporal relation extraction. *CoRR*, 2025c.

Zhao, X., Pang, W., Xue, Z., Jian, X., Zhang, L., Xu, Y., Song, X., Wu, S., and Yu, T. The underappreciated power of vision models for graph structural understanding. *CoRR*, 2025d.

Zhu, Y., Bai, X., Chen, K., Xiang, Y., Yu, J., and Zhang, M. Benchmarking and improving large vision-language models for fundamental visual graph understanding and reasoning. In *ACL*, 2025.

## Appendix

### A. Empirical Motivation: Recurrence of Structural Motifs Across Domains

This appendix provides empirical motivation for the representation-centric perspective in Section 2.1. We analyze whether coarse structural motifs recur across heterogeneous domains when relational structure is expressed as graph states, i.e., sets of relational tuples  $\mathcal{G} = \{(u, r, v)\}$ . Our goal is to verify that (i) simple local motifs (e.g., two-hop chains and hub structures) appear consistently across domains, while (ii) global structural scales (e.g., path lengths) can vary in a domain-dependent but interpretable manner.

#### A.1. Datasets and Graph View

We analyze four domains used throughout the paper: graph algorithm (Wei et al., 2024; Wang et al., 2024b), molecular graph description (Fang et al., 2024), scene graph generation (Krishna et al., 2017), and event relation extraction (Wang et al., 2022; Glavas et al., 2014). Each instance is treated as a *graph state* represented by a set of relational tuples. For this analysis, we abstract away task semantics and focus purely on topology-level structure; when required by the metric, directed graphs are converted to an undirected view.

#### A.2. Structural Statistics

We report four topology-level statistics that characterize coarse structural properties shared across domains: (1) **AvgDeg**: the mean node degree per graph (computed on the undirected view), capturing *relational density*; (2) **ASPL**: the average shortest path length per graph (undirected), capturing *global connectivity scale*; (3) **TwoHop**: the average number of length-2 paths ( $A \rightarrow B \rightarrow C$ ) per graph, capturing the prevalence of *two-step compositional dependencies*; (4) **Star**: the average number of hub nodes (degree  $\geq 3$ ) per graph, capturing *hub-centric* relational organization. All statistics are computed by first aggregating counts within each graph and then averaging over the dataset.

Domain	AvgDeg $\uparrow$	ASPL	TwoHop $\uparrow$	Star $\uparrow$
Graph Algorithm	5.8068	2.0787	632.7410	16.1844
Molecular Graph Description	2.1125	6.1799	52.5278	11.9700
Scene Graph Generation	1.5111	1.4485	2.4198	0.7078
Event Relation Extraction	1.4739	1.3731	14.9518	0.8642

Table 5. Topology-level structural statistics across four domains. AvgDeg and ASPL are per-graph averages computed on undirected views. TwoHop and Star quantify the prevalence of two-hop chains and hub nodes, respectively. These statistics are reported only to establish the recurrence of coarse structural patterns across domains, rather than to compare magnitudes or evaluate models.

**Cross-domain observations.** Table 5 reveals two complementary patterns. First, **local structural motifs recur broadly across domains**: all four settings exhibit non-trivial two-hop dependencies and hub nodes, indicating that compositional relational structure is not confined to any single modality or task formulation. Second, **global structural scale varies in an interpretable manner**. Molecular graphs exhibit substantially larger ASPL, consistent with their chain-like or near-tree chemical backbones. Algorithmic graphs are denser and contain many more two-hop dependencies, reflecting larger graph sizes and higher branching factors. In contrast, event and scene graphs are comparatively compact ( $ASPL \approx 1.4$ ) with similar relational density ( $AvgDeg \approx 1.5$ ), suggesting that compact relational organization can arise across both textual (event-centric) and visual (scene-centric) sources.

#### A.3. Qualitative Evidence of Shared Structural Constraints Across Tasks

To further clarify how graph structure functions as a reusable substrate across heterogeneous tasks, we present qualitative evidence showing that *structurally identical motifs not only recur across domains, but also encode closely aligned constraint roles*. Specifically, we pair instances from **event graphs** (text-derived) and **scene graphs** (vision-derived) that instantiate the same coarse structural templates, and show that these templates impose similar relational constraints despite differences in semantics and relation inventories.

Throughout this section, motif identity is defined purely at the level of *topology* rather than label semantics. Our goal is not to establish semantic equivalence, but to demonstrate that shared structural forms correspond to shared constraint interpretations across tasks.

**Two-hop chains ( $A \rightarrow B \rightarrow C$ ).** We first examine two-hop chains, which represent the minimal form of compositional relational structure. Across both domains, all examples instantiate the same role-aligned structural template:

$$\boxed{A} \rightarrow \boxed{B} \rightarrow \boxed{C}$$

*Constraint role:* an intermediate state  $B$  composes two relations, imposing a mediated dependency between a source  $A$  and an outcome  $C$ .

Event graph (text)	Scene graph (vision)	Aligned constraint role
$E7 : took\_place \rightarrow E3 : ridden \rightarrow E2 : remounted$	$board \rightarrow fence \rightarrow zebra$	Mediated dependency via an intermediate anchor
$E13 : received \rightarrow E3 : believed \rightarrow E31 : appeared$	$board \rightarrow counter \rightarrow bowl$	Composition of two relations through $B$
$E10 : gained \rightarrow E31 : published \rightarrow E18 : avalanches$	$engine \rightarrow train \rightarrow track$	Two-step mediated relational path

Table 6. Cross-domain two-hop chain pairs. Although event and scene graphs differ in semantics and relation types, both instantiate the same compositional constraint: an intermediate node mediates dependencies between a source and an outcome.

Across all pairs, the identity of the intermediate node  $B$  differs in meaning (e.g., temporal anchoring in event graphs versus spatial mediation in scene graphs), yet its *structural role* remains invariant: it serves as a compositional bottleneck that constrains how two relations interact. This consistency highlights that two-hop chains encode similar constraint semantics across tasks.

**Hub / star motifs (degree  $\geq 3$ ).** We next examine hub motifs, which capture cases where a single node participates in many relations. Across both domains, these instances instantiate the same star-like template:

$$\boxed{H} \leftrightarrow \{n_i\}_{i=1}^k, \quad k = \deg(H)$$

*Constraint role:* a shared anchor  $H$  simultaneously constrains multiple relations, enforcing global consistency across dependent nodes. In both event and scene graphs, hub nodes function as structural anchors rather than task-specific artifacts. They concentrate relational

Event graph			Scene graph			Aligned constraint role
Hub	Deg	Rel. type	Hub	Deg	Rel. type	
$E6 : received$	4	temporal	$counter$	3	spatial/support	Central anchor for multiple relations
$E3 : ridden$	6	temporal	$guy$	5	part-of/attribute	Shared reference point across dependents
$E31 : published$	20	temporal	$train$	6	part-of/spatial	Shared anchor coordinating multiple relations

Table 7. Cross-domain hub motif pairs with aligned constraint interpretations. Despite different relation semantics, hubs in both domains act as shared anchors that impose multi-relation consistency.

constraints around a central node, allowing multiple relations to be coordinated through a shared reference point. This role remains consistent even though the surrounding relations encode different semantics (temporal, spatial, or part-of).

Together, these paired examples demonstrate that recurring structural motifs across tasks encode not only similar topological patterns, but also closely aligned *constraint roles*. This observation supports the representation-centric view adopted in Section 2.1: graph structure operates as a reusable intermediate substrate at the level of relational organization, abstracting away from task- or modality-specific semantics while preserving constraint-level meaning.

## B. Concrete Instantiation of the Unified Graph Representation

This section provides a concrete instantiation of the shared graph representation described in Section 2.1. The goal of this instantiation is not to prescribe a canonical graph format, but to illustrate one practical realization of the structural form used in **G-Substrate**.

In our experiments, each graph is represented as a collection of uniquely identified entities and typed, directed relations defined over ordered pairs of entities. Optional attributes may be attached to entities or relations when required by specific tasks, but are treated as auxiliary annotations and do not modify the underlying relational topology. Structural identity is therefore determined solely by relational connectivity, which is the property that must remain stable for graphs to be reusable across tasks and functional roles.

This structural form is used uniformly across tasks without encoding task-specific semantics, execution procedures, or optimization objectives. The same graph may be consumed as an intermediate representation in graph understanding tasks or produced as an output in graph generation tasks. Differences between tasks are expressed through prompts, supervision signals, and evaluation protocols, rather than through modifications to the graph structure itself.

We emphasize that this instantiation represents only one possible realization of the shared graph representation. **G-Substrate** does not depend on any particular schema choice, serialization format, or internal encoding, as long as graphs conform to a consistent entity–relation structural form that enables reuse across tasks.

## Graph is a Substrate Across Data Modalities

Component	Field	Description
Entity	id	Unique entity identifier (e.g., E1, E2)
	type	Optional entity category or label
Relation	subject	Source entity identifier
	predicate	Typed relation label
	object	Target entity identifier
Attribute	key	Optional attribute name
	value	Attribute value

Table 8. Minimal structural primitives used in one realization of the shared graph representation.

**Graph representations across domains.** Although instantiated in different domains, all graphs used in our experiments conform to the same entity–relation abstraction: uniquely identified entities connected by typed relations over ordered pairs, with optional auxiliary attributes.

Domain	Entity Example	Relation Example	Structural Role
Graph Algorithmic	node id (e.g., 5, 17)	CONNECTED	Pure topology
Molecular Graph	atom (C, O, C <sub>aromatic</sub> )	SINGLE-BOND, AROMATIC-BOND	Chemical interaction structure
Event Graph	event mention ( <i>destroyed</i> , <i>displaced</i> )	BEFORE, AFTER	Temporal / causal dependency
Scene Graph	object / part (cat, box, eye)	ON, HAS, OF	Spatial / semantic interaction

Table 9. Examples of how different domains instantiate the same entity–relation structural abstraction. Variation lies in label vocabularies and supervision, while the relational form remains consistent.

Across domains, variation lies in label vocabularies and supervision protocols rather than in structural form. Structural identity is determined solely by relational connectivity over entity identifiers, enabling graphs to be reused across tasks with different functional roles without structural translation. While G-Substrate does not rely on any specific representation choice for its validity, different realizations may induce different inductive biases and therefore lead to quantitative differences in downstream performance. We empirically study this effect in Section 3.

## C. Task Coverage and Framework Instantiation

This section summarizes how the **G-Substrate** framework is instantiated across different task settings. Rather than enumerating dataset-specific configurations, we focus on how graph representations are generated, understood, and reused across tasks under the structural substrate defined in the main text.

Task Setting	Input Modality	Graph Role	Reuse Pattern
Scene Graph Generation	Image	Generation	–
Event Relation Extraction	Text	Generation	–
Molecular Graph Description	Structured Molecule Input	Unstanding	–
Graph Algorithm Task	Graph	Unstanding	Reuses graphs produced in scene graph generation and event relation extraction
Subgraph Retrieve Task	Graph	Unstanding	Reuses graphs produced in scene graph generation and event relation extraction
Cross-Modal Consistency	Image + Graph	Unstanding	Bidirectional reuse between perception and structure

Across the task instantiations considered in this work, graphs satisfy the same structural admissibility constraints defined by the unified schema, allowing Graph generated in one setting to remain structurally compatible with others. Differences between tasks arise from how graphs are generated and understood, rather than from changes to the underlying structural constraints. For cross-modal consistency tasks, we additionally introduce controlled structural perturbations to a subset of the reused graph to construct negative examples. These perturbations modify relational connectivity while preserving surface-level elements, enabling the model to distinguish structurally coherent graphs from inconsistent ones. This design ensures that consistent supervision provides meaningful structural learning signals rather than relying solely on positive reuse cases.

## D. Training Paradigm Definitions

This section provides operational definitions of the training paradigms summarized in Section 3.2. All paradigms use the same backbone model, optimizer, training schedule, data mixture, and total training budget. They differ only in (i) the representational constraints applied to graph states and (ii) how graph states are exposed to functional roles during training.

**Naive single-task.** Each task is trained independently using its original task-specific graph representation and supervision objective. Training batches contain examples from a single task only, and graph states are constructed, optimized, and consumed exclusively in that task. Graphs are optimized under a single functional role, and no cross-role exposure occurs.

**Unified single-task.** Each task remains trained in isolation, but graphs are represented using the unified structural schema described in Section 2.2. Although the same structural admissibility constraints apply across tasks, graphs are never exposed outside their originating task. Learning signals remain task-specific, and graphs still operate under a single functional role, so no reuse pressure is present.

**Naive multi-task.** All tasks are jointly trained by sampling batches from multiple tasks under their native graph formats. Model parameters are updated across tasks, but graphs are still constructed and can be understood only in their originating tasks. Graphs are therefore optimized under task-specific roles, without structural alignment or cross-role reuse.

**Unified multi-task (schema only).** Tasks are jointly trained while graphs are expressed using the unified structural schema. This imposes a common set of structural admissibility constraints across tasks, aligning graph representations at the structural level. However, graphs remain tied to their task of origin and are not exposed to different functional roles. Structural compatibility is established, but no cross-role reuse occurs.

**Naive multi-task + interleave.** Interleaved role-based training is introduced: the graph produced under one task-role instantiation may be reused as inputs under another task-role instantiation. This exposes the same graph state to multiple functional roles during training. However, graphs retain their task-specific formats, and no unified structural admissibility constraint is imposed. Cross-role reuse occurs, but under heterogeneous structural conventions.

**G-Substrate (Unified + interleave).** Our full framework combines the unified structural schema with interleaved role-based training. Graphs satisfy a common set of structural admissibility constraints and are explicitly reused under multiple functional roles during training. Learning, therefore, applies consistent pressure toward graph representations that remain structurally compatible and reusable across heterogeneous task contexts.

## E. Hyperparameter Configuration

Table 10 summarizes the shared hyperparameter configuration used across all experiments, including task-isolated training, naive multi-task learning, and the proposed **G-Substrate** framework. All compared methods use identical model backbones, optimization settings, training budgets, and decoding configurations. All experiments are performed on a server with four NVIDIA A100 GPUs (40GB each). Fine-tuning is implemented using the LLaMA-Factory framework.

Hyperparameter	Value
Backbone models	Qwen3-VL-2B
Finetuning type	Full-parameter training
Vision tower frozen	Yes
MM projector frozen	No
Language model frozen	No
Optimizer	AdamW ( $\beta_1=0.9, \beta_2=0.98$ )
Learning rate	$8 \times 10^{-6}$
Weight decay	0.01
Learning rate schedule	Cosine decay
Warmup ratio	0.10
Max input length	2048 tokens
Mixed precision	bfloat16
Per-device batch size	1
Gradient accumulation steps	32
Effective batch size	64 sequences
Training epochs	2
Max gradient norm	1.0
Random seed	42
Decoding strategy	Greedy decoding (temperature = 0)

Table 10. Shared training configuration used across experiments unless otherwise specified.

## F. Detailed Experimental Results

This appendix reports detailed results under different training paradigms of our framework, providing per-task and per-dataset breakdowns that complement the main experimental findings.

The details from table 11 to table 14 results across domains reveal a consistent interaction between representation format and training

Graph is a Substrate Across Data Modalities

Method	Connectivity	Cycle	Shortest Path	Matching	Overall
Naive single-task	99.44	92.18	38.27	92.05	92.89
Unified single-task	97.80	94.72	37.14	85.98	90.43
Naive multi-task	99.71	94.72	41.27	92.21	93.01
Unified multi-task	98.09	96.19	45.02	94.23	93.85
Naive multi-task + interleave	98.27	93.86	43.83	91.92	93.24
G-Substrate	98.41	96.97	48.59	94.54	94.47

Table 11. Detailed results on graph algorithmic tasks.

Method	BLEU-4	ROUGE-L
Naive single-task	48.59	66.65
Unified single-task	47.35	65.64
Naive multi-task	48.11	66.11
Unified multi-task	49.99	67.36
Naive multi-task + interleave	48.63	64.98
G-Substrate	51.53	68.47

Table 12. Detailed results on molecular graph description.

Method	PCIs R@50	PCIs mR@50	SGCLs R@50	SGCLs mR@50
Naive single-task	23.74	7.78	11.95	4.10
Unified single-task	22.43	5.84	10.43	4.01
Naive multi-task	24.68	7.49	13.57	4.00
Unified multi-task	24.71	7.00	13.78	4.80
Naive multi-task + interleave	24.02	7.64	13.24	4.30
G-Substrate	25.38	8.67	14.07	5.30

Table 13. Detailed results on scene graph generation.

Method	MAVEN-ERE									HiEve		
	Subevent			Temporal			Causal			P	R	F1
	P	R	F1	P	R	F1	P	R	F1	P	R	F1
Naive single-task	43.44	42.27	39.65	39.05	55.22	41.60	31.45	30.87	27.70	15.10	30.95	17.10
Unified single-task	52.80	44.63	45.45	37.84	42.79	33.29	38.07	29.45	30.22	13.14	21.83	14.28
Naive multi-task	40.44	39.27	36.87	37.05	53.22	39.14	37.45	37.87	37.02	15.29	30.41	18.78
Unified multi-task	56.36	53.52	51.89	44.74	48.84	40.05	45.41	43.53	40.75	18.34	25.38	19.37
Naive multi-task + interleave	50.43	47.32	45.74	39.41	42.89	38.86	41.44	43.24	37.99	20.43	24.74	21.36
G-Substrate	58.91	52.18	52.20	46.98	51.69	42.68	48.89	40.09	40.91	22.25	35.74	25.15

Table 14. Event relation extraction results on MAVEN-ERE and HiEve.

organization. In task-isolated settings, enforcing the unified schema alone does not yield gains and can even reduce performance, as structural constraints are not exercised beyond a single objective. Under multi-task learning, however, unified representations become beneficial, indicating that structural alignment matters once graph states are exposed to multiple learning contexts. The full G-Substrate framework further improves over both naive and unified multi-task baselines, with the largest gains observed in tasks that rely on multi-step relational composition, such as shortest-path reasoning, rare scene-graph relations, and event substructure modeling. By contrast, naive interleaving without schema-level alignment provides only limited and unstable improvements. These patterns suggest that performance gains arise not from task mixing alone, but from organizing learning so that structurally admissible graph states are reused across heterogeneous roles.

## G. Generality Across Model Backbones

To examine whether the observed performance gains are specific to a particular vision–language model backbone, we conduct a lightweight transfer study using an alternative vision–language model backbone from a different model family. This analysis is intended as a robustness check rather than an exhaustive model comparison.

We repeat a subset of the main experiments using InternVL3.5-2B-HF under the same training recipe, data composition, and evaluation protocol as in the main paper. Specifically, we compare task-isolated training, naive multi-task learning, and the full **G-Substrate** framework, along with key component ablations.

Method	GAR				MGD		SGG		ERE			
	CT	CD	SP	BM	BLEU-4	ROUGE-L	PCIs	MA-S	MA-T	MA-C	HiE	
Naive single-task	<b>99.65</b>	94.22	37.33	92.36	50.37	67.60	26.94	41.68	42.80	32.87	16.70	
Unified single-task	97.86	94.29	36.96	92.36	49.89	67.44	28.15	52.65	37.82	34.80	10.74	
Naive multi-task	<b>99.84</b>	95.42	45.81	92.67	51.45	68.28	26.59	43.40	<u>43.84</u>	32.47	18.22	
Unified multi-task	98.26	<u>95.98</u>	47.46	<u>94.39</u>	51.77	68.77	28.29	<b>57.04</b>	<b>45.62</b>	<b>41.57</b>	18.78	
Naive multi-task + interleave	98.04	94.86	46.89	93.48	51.63	67.98	28.02	53.74	38.94	38.74	21.36	
<b>G-Substrate</b>	98.28	<b>98.28</b>	<b>50.65</b>	<b>94.54</b>	<b>52.02</b>	<b>68.95</b>	<b>29.01</b>	55.23	43.04	39.05	<b>21.68</b>	

Table 15. Task-level performance using an alternative model backbone (InternVL). The same training recipe and evaluation metrics as in the main experiments are used. Best results are in **bold**; second-best are underlined.

Table 15 shows that the overall trends observed in the main experiments persist under a different model backbone. In task-isolated settings, the unified schema alone does not consistently outperform native representations, and in some cases slightly reduces performance, mirroring the behavior observed with the primary backbone. This again indicates that structural alignment by itself does not constitute an intrinsic performance advantage. Under multi-task training, however, unified representations become more effective. Unified multi-task learning improves over naive multi-task training across most domains, particularly in shortest-path reasoning (SP), scene graph metrics, and event relation extraction. The full G-Substrate framework further improves over both baselines, yielding the strongest or near-strongest results in most settings. Notably, gains are most visible in tasks that require multi-step relational composition, such as SP in GAR and subevent/causal relations in ERE, which are structurally similar to the patterns seen with the original backbone. Naive multi-task with interleaving provides partial benefits but remains less stable across domains, especially in ERE, where some metrics degrade relative to unified multi-task training. This again suggests that cross-task exposure alone is insufficient, and that consistent structural admissibility plays an important role in enabling reliable reuse.

Overall, the consistency of these patterns across two architecturally distinct vision–language backbones indicate that the improvements are not tied to a specific model family. Instead, they stem from how relational structure is represented and reused during training, supporting the generality of the framework.

## H. Extended Related Work

This appendix expands the discussion in Section 4 and situates our work within a broader landscape of research involving graph structure in learning systems. We organize prior work according to a common task formulations in which graphs arise, and analyze how graph representations are constructed, optimized, and used. Across these paradigms, a recurring pattern emerges: graph structure is typically introduced to satisfy the objective of an individual task, and is rarely maintained as a persistent intermediate representation that must remain compatible and reusable across tasks.

### H.1. Tasks over Structured Graphs with LLMs and VLMs

A substantial body of work studies tasks defined over structured graph inputs using LLMs and VLMs. These include graph-theoretic reasoning and algorithmic problems such as shortest path, connectivity, traversal, and combinatorial queries, often realized through graph serialization, specialized prompting, or graph-aware tokenization strategies (Li et al., 2025b; Hu et al., 2025c; Chen et al., 2024b; Wang et al., 2024b; 2023; Yuan et al., 2025b; Zhang et al., 2024b; Tang et al., 2024b; Wang et al., 2025a; Bi et al., 2025c). More recent work extends such settings to multimodal regimes, where graphs are derived from images or other perceptual signals and processed by VLMs (Wei et al., 2024; Sartori et al., 2025; Li et al., 2024b; Zhu et al., 2025; Zhao et al., 2025b;d; Bi et al., 2025a;b). Related efforts address tasks such as molecular graph description and reasoning, where structured graphs are mapped to semantic outputs (Kim et al., 2025; Liu et al., 2024c; Park et al., 2024; Fang et al., 2024; Yin et al., 2025; Luo et al., 2024b; Wu et al., 2025b; Jin et al., 2025).

Across these works, the graph is typically treated as a task-bounded input object. Its representation is optimized only insofar as it supports the current objective (e.g., algorithmic prediction or description generation). There is no requirement that graph representations remain structurally compatible with other tasks, nor that they serve as intermediate artifacts reused under different learning roles.

### H.2. Graph Generation in Vision and Language

Another major line of work focuses on generating graphs from perceptual or linguistic inputs, such as scene graph generation from images (Chen et al., 2024d; Li et al., 2024a; Liu et al., 2025; Xu et al., 2025c; Hu et al., 2025b; Min et al., 2025; Hu et al., 2025a; Wang et al., 2025c; Elskhawy et al., 2025; Chen et al., 2025b; Dutta et al., 2025; Hu et al., 2025d; Kong & Zhang, 2025; Li et al., 2025c) and event–event relation extraction from text (Hu et al., 2025e; Xu et al., 2025b; Chen et al., 2024b; Ding et al., 2025; Zhao et al., 2025c; Tanev et al., 2025; Li et al., 2025a; Wang et al., 2024d; Liu & Wang, 2025; Chen et al., 2024a). In these formulations, graphs serve as final prediction targets. Training objectives optimize graph quality with respect to task-specific metrics, and the Generated graphs are evaluated independently within each task context.

As a result, graphs are not required to persist beyond generation or to function as reusable intermediate representations for other tasks.

Structural regularities learned during generation are not explicitly constrained to remain compatible with graph-conditioned reasoning tasks.

### **H.3. Multi-Task and Multi-Modal Learning**

Multi-task and multi-modal learning have been extensively studied as mechanisms for coordinating learning across tasks and modalities (Ruder, 2017; Akhtar et al., 2020; Yuan et al., 2025a; Zhang & Yang, 2022). Typical approaches emphasize parameter sharing (Pan et al., 2025; Liu et al., 2024a; Leng & Xiong, 2025), task balancing (Xia et al., 2024; Zhao et al., 2025a; Gong et al., 2024; Ju et al.), curriculum design (Chen et al., 2025a; Zhao et al., 2025a; Wang et al., 2024c), and optimization heuristics (Xia et al., 2024; Zhang et al., 2025; Leng & Xiong, 2025).

These methods coordinate learning at the level of parameters, losses, or data scheduling. When the graph structure appears, it is embedded within task-specific inputs or outputs, and reuse occurs implicitly through parameter sharing rather than through explicit constraints on intermediate representations. Graph structures themselves are not treated as objects that must remain structurally valid across heterogeneous task roles.

### **H.4. Unified and Foundation Graph Models**

Graph foundation models aim to build general-purpose systems that transfer across graph tasks and domains through large-scale pretraining, architectural unification, and broad task coverage. Existing approaches can be broadly categorized into three directions: *graph-model-centric* methods that extend graph neural architectures toward broader generality (Liu et al., 2024b; Wang et al., 2024f; e; Yu et al., 2024; Jiang et al., 2024); *language-model-centric* methods that adapt LLMs to operate on graph-structured inputs or tasks (Li et al., 2025b; Lin et al., 2024; Kong et al., 2025; Wang et al., 2024b); and *joint graph-language pretraining* approaches that co-train graph and language representations within a unified frameworks (Tang et al., 2024a; Luo et al., 2024a; Chen et al., 2024c; Zhang et al., 2024a; Liu et al., 2024d; Wang et al., 2024a; Hu et al., 2024; Wang et al., 2025e; Liu et al., 2023; Wang et al., 2025d; Thapaliya et al., 2025; Ma et al., 2025). These models emphasize scale, pretraining diversity, and architectural unification, aiming to improve transfer across graph tasks through shared parameters and large training corpora. However, the graph structure in these systems remains conditioned on task formulations: graph representations are constructed and optimized with respect to individual task objectives, and are not required to persist as intermediate artifacts beyond the originating task.

Our work explores a complementary axis of generalization. Rather than focusing on how parameters or model architectures generalize across tasks, we study how *intermediate graph states themselves* can be organized to remain structurally admissible and reusable under heterogeneous task roles. We explicitly enforce structural compatibility and cross-task reuse of the graph states, treating graphs as a reusable substrate in the learning process rather than as task-bound artifacts. This perspective is orthogonal to scaling and architectural unification, and addresses how structured representations persist and function across learning contexts.